Title

miR-29 Sustains B Cell Survival and Controls Terminal Differentiation via Regulation of PI3K Signaling

Journal

Cell Reports, 33(9)

ISSN

2639-1856

Authors

Hines, Marcus J
Coffre, Maryaline
Mudianto, Tenny
et al.

Publication Date

2020-12-01

DOI

10.1016/j.celrep.2020.108436

Peer reviewed

HHS Public Access

Author manuscript

Cell Rep. Author manuscript; available in PMC 2020 December 11.

Published in final edited form as:

Cell Rep. 2020 December 01; 33(9): 108436. doi:10.1016/j.celrep.2020.108436.

miR-29 Sustains B Cell Survival and Controls Terminal Differentiation via Regulation of PI3K Signaling

Marcus J. Hines[1], **Maryaline Coffre**[1], **Tenny Mudianto**[1], **Marisella Panduro**[2,3], **Eric J. Wigton**[2,3], **Cosmin Tegla**[1], **Victoria Osorio-Vasquez**[1], **Robin Kageyama**[2,3], **David Benhamou**[5], **Oriana Perez**[1], **Sofia Bajwa**[1], **Michael T. McManus**[2,4], **K. Mark Ansel**[2,3], **Doron Melamed**[5,*], **Sergei B. Koralov**[1,6,*]

[1]Department of Pathology, NYU School of Medicine, New York, NY 10016, USA

[2]Department of Microbiology and Immunology, UCSF, San Francisco, CA 94143, USA

[3]Sandler Asthma Basic Research Center, UCSF, San Francisco, CA 94143, USA

[4]Diabetes Center, UCSF, San Francisco, CA 94143, USA

[5]Department of Immunology, Faculty of Medicine, Technion, Haifa 31096, Israel

[6]Lead Contact

SUMMARY

The phosphatidylinositol 3-kinase (PI3K) signaling cascade downstream of the B cell receptor (BCR) signalosome is essential for B cell maturation. Proper signaling strength is maintained through the PI3K negative regulator phosphatase and tensin homolog (PTEN). Although a role for microRNA (miRNA)-dependent control of the PTEN-PI3K axis has been described, the contribution of individual miRNAs to the regulation of this crucial signaling modality in mature B lymphocytes remains to be elucidated. Our analyses reveal that ablation of miR-29 specifically in B lymphocytes results in an increase in PTEN expression and dampening of the PI3K pathway in mature B cells. This dysregulation has a profound impact on the survival of B lymphocytes and results in increased class switch recombination and decreased plasma cell differentiation. Furthermore, we demonstrate that ablation of one copy of *Pten* is sufficient to ameliorate the phenotypes associated with miR-29 loss. Our data suggest a critical role for the miR-29-PTEN-PI3K regulatory axis in mature B lymphocytes.

Graphical Abstract

*Correspondence: melamedd@tx.technion.ac.il (D.M.), sergei.koralov@nyumc.org (S.B.K.).

AUTHOR CONTRIBUTIONS

M.J.H. and S.B.K. performed and designed experiments, analyzed the data, and wrote the manuscript. E.J.W., T.M., C.T., V.O.-V., D.B., O.P., and S.B. performed experiments and/or contributed to analysis. M.P., R.K., M.T.M., and K.M.A. developed the gene-targeted animals used for this project and provided scientific input. M.C. contributed to experimental design and participated in the preparation of the manuscript. D.M. contributed to experimental design and project development.

SUPPLEMENTAL INFORMATION

Supplemental Information can be found online at https://doi.org/10.1016/j.celrep.2020.108436.

DECLARATION OF INTERESTS

The authors declare no competing interests.

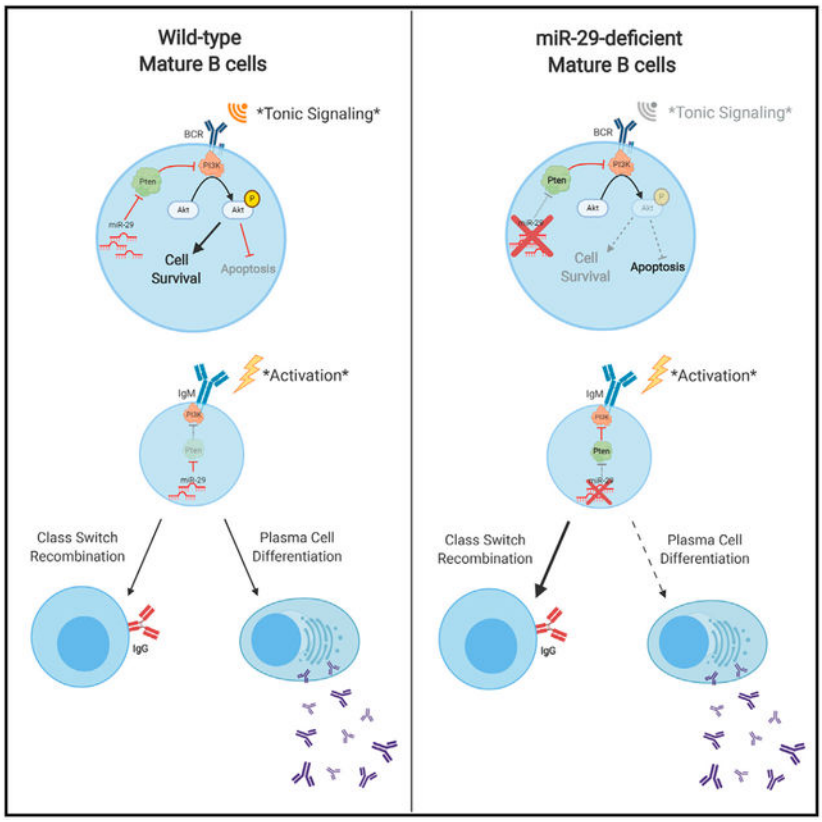

In Brief

Hines et al. report that miR-29 in murine B lymphocytes regulates the BCR-PI3K signaling cascade by dampening PTEN expression and that loss of this miRNA cluster results in increased apoptosis as well as defects in B cell terminal differentiation.

INTRODUCTION

The phosphoinositide 3-kinase (PI3K) cascade is a ubiquitously expressed signal transduction pathway that promotes the survival, proliferation, and metabolism of cells (Engelman et al., 2006; Liu et al., 2009; Vanhaesebroeck et al., 2010). Essential for signal transduction downstream of the B cell receptor (BCR) in mature lymphocytes and pre-BCR in developing cells, PI3K orchestrates B cell development and is important for maintaining B cell identity (Abdelrasoul et al., 2018; Clayton et al., 2002; Fruman et al., 1999; Okkenhaug et al., 2002; Ramadani et al., 2010). The maintenance of an appropriate signal from the PI3K pathway for B cells is vital. Low-amplitude PI3K “tonic” signal is essential for the survival of B lymphocytes, as inhibition of key proteins in the PI3K pathway leads to apoptosis (Okkenhaug, 2013; Srinivasan et al., 2009), whereas overactivation of this pathway in B cells can lead to developmental defects and is associated with malignant transformations (Avery et al., 2018; Thorpe et al., 2015). Because of its negative effects on the PI3K pathway, phosphatase and tensin homolog (PTEN) is recognized as a critical tumor

suppressor and has been shown to prevent cells from proliferating or growing (Kwabi-Addo et al., 2001; Stambolic et al., 1998; Sun et al., 1999; Wang et al., 2003).

The post-transcriptional regulation of PTEN expression by microRNAs (miRNAs) is crucial for maintaining essential homeostasis of PI3K signaling. miRNAs are evolutionarily conserved, small non-coding RNAs of ~22 nucleotides that guide the RNA-induced silencing complex (RISC) to target the 3′ UTR of mRNA transcripts for translational repression or degradation (Krol et al., 2010; Wilson and Doudna, 2013; Winter et al., 2009). We have previously shown that deleting the enzymes responsible for miRNA biogenesis in B cells leads to an increase in PTEN expression, increased apoptosis, and developmental defects (Coffre et al., 2016; Koralov et al., 2008). Furthermore, a number of individual miRNAs have been implicated in the regulation of the PTEN-PI3K axis in developing B cells in the bone marrow (Benhamou et al., 2016; Chen et al., 2004; Koralov et al., 2008; Lai et al., 2016; Ventura et al., 2008; Xiao et al., 2008). However, which miRNAs are responsible for modulation of the PTEN-PI3K axis in mature B cells remains to be elucidated.

The miR-29 family of miRNAs is highly expressed in the adaptive immune system (Landgraf et al., 2007; Liston et al., 2012) and has previously been shown to regulate PTEN expression in different cell types (Kong et al., 2011; Shen et al., 2016; Tumaneng et al., 2012; Wang et al., 2013), but our understanding of its role in lymphocytes remains fragmentary. In the present study, we investigate the role of miR-29 in regulating the PTEN-PI3K axis within mature B cells and reveal the implications of this regulatory axis for B cell survival and terminal differentiation. By analyzing mice in which both miR-29 loci are ablated selectively in B cells, we demonstrate an increase in intracellular PTEN levels accompanied by a dampening of the PI3K signaling cascade. These mice exhibited a significant decrease in splenic mature B cells with a corresponding increase in apoptosis. Additionally, isolated B cells preferentially underwent class switch recombination over plasma cell differentiation *in vitro* and *in vivo*. Deletion of one allele of *Pten* in miR-29 null B cells led to a partial rescue of B cell survival and reverted the differentiation pheno-type. Our data suggest a critical role for miR-29 in maintaining the homeostasis of PI3K signaling by post-transcriptional regulation of PTEN in mature B cells.

RESULTS

Loss of Mature Follicular B Cells in miR-29-Deficient Mice Due to Apoptosis

The mmu-miR-29 family of miRNAs originate from genes at two different loci: *miR-29ab1* on chromosome 6 and *miR-29b2c* on chromosome 1. These genes encode three mature products, namely, miR-29a, miR-29b, and miR-29c, that share identical seed regions, which allow them to target the same mRNA transcripts. Simultaneous germline disruption of both alleles has been reported to lead to early postnatal lethality in miR-29 null mice (Cushing et al., 2015), and although no obvious developmental defects were described in these animals, we found that in our hands, virtually no miR-29 null mice survived to weaning age (data not shown). To examine the role miR-29 plays in B cell survival and function, we used B-cell-specific miR-29ab1 knockout (KO) (mb1Cre/+ miR-29ab1$^{fl/fl}$), along with global miR-29b2cKO (miR-29b2c$^{-/-}$; Smith et al., 2012) and double-KO (DKO; mb1Cre/+

miR-29ab1$^{fl/fl}$ miR-29b2c$^{-/-}$) mouse models. RT-PCR analyses of mature B cells revealed dramatic diminution of each miR-29 family member in DKO mice with no significant effect on other miRNAs (Figure 1A). Analyses of ab1KO and b2cKO mice revealed significant downregulation of miR-29a and miR-29c, respectively (Figure S1A).

To examine the impact of miR-29 loss on B cells, we analyzed spleens from DKO mice. Analyses revealed a decrease in the percentage of splenic B cells and a stark decrease in the total count of B cells in the DKO mice (Figures 1B and S1B). We observed milder decreases in the percentage of splenic B cells and total B cell numbers in the single miR-29 cluster KO mouse models (Figure S1B). Additionally, Annexin V staining revealed an increase in apoptosis of B cells from DKO mice compared to controls (Figures 1C and 1D). These findings were corroborated with intracellular caspase staining (Figure S1C). The loss of B cells in the DKO mice was largely attributed to a reduction in mature B cell numbers and a modest decrease in immature B cells (Figures S1D and S1E). The mature B cell compartment is comprised of marginal zone (MZ) B cells that undergo T-independent differentiation and follicular (FO) B cells that undergo T-dependent differentiation in germinal centers (Hoffman et al., 2016). Within the mature compartment of the DKO mouse model, the decrease in B cells appeared to be largely due to the apoptosis of FO B cells, with only a modest loss in total MZ B cell numbers (Figures 1E, 1F, S1F, and S1G).

To ensure that the diminution of B cells in DKO mice was not a consequence of altered B cell development, we analyzed bone marrow from DKO and control mice. Our analyses revealed no differences in pro-, pre-, or immature B cells compared with littermate controls (Figures S2A–S2F). Recirculating mature B cells that cycle back through the bone marrow (Fairfax et al., 2008) were significantly reduced, corresponding with the decrease in mature B cells in the periphery (Figure S2G). These findings suggest that the DKO mice are able to produce B cells efficiently and that the loss of peripheral B cells is a consequence of dysregulation in mature B cell subsets.

miR-29 Targets the 3′ UTR of PTEN Later in B Cell Development

A sequence-based miRNA binding site assessment (TargetScan, PicTar, and miRanda) within the murine PTEN 3′ UTR revealed two highly conserved binding sites for miR-29 (Figure 2A). Furthermore, analysis of miR-29 expression along the developmental stages of B lymphocytes from C57BL/6 mice established an inverse pattern of expression of this cluster to miR-17~92, a known PTEN regulator (Benhamou et al., 2016). miR-17~92 expression peaked at the pro-B cell stage and steadily declined as the B cell matured (Figure 2B). Conversely, miR-29 increased as the B cell matured—peaking at the FO B cell stage (Figure 2B). Summed normalized counts of the miR-17~92 cluster and miR-29 family from RNA sequencing (RNA-seq) data performed by Spierings et al. (2011) corroborated our RT-PCR-based quantification (Figure S3A). This finding suggested that although miR-17~92 is critical for early B cell development, miR-29 may be a crucial regulator of the PTEN-PI3K signaling cascade in mature B cells.

We took advantage of the Renilla luciferase dual reporter system to investigate whether miR-29 directly targets PTEN transcripts. To validate a sequence-specific miRNA-target relationship, we introduced either an intact 2-kb fragment of the 3′ UTR of PTEN or a

sequence with miR-29 sites mutated downstream of Renilla luciferase cDNA (Rhluc) (Figure 2C). The mutant versions of the construct contained miR-29 sites with the binding sequence altered such that neither miR-29 nor other known miRNAs could bind and allowed us to dissect the contribution of the two putative miRNA binding sites to the regulation of PTEN expression. Co-transfecting the wild-type (WT) reporter plasmid with a miR-29a, miR-29b, or miR-29c mimic resulted in a significant reduction in Renilla/luciferase activity and revealed that both sites could contribute to the regulation of the PTEN transcript (Figure 2D). An analysis of a recently published Argonaute high-throughput sequencing of RNA isolated by crosslinking immunoprecipitation (Ago HITS-CLIP) dataset from activated mature B cells of C57BL/6 mice demonstrated RISC binding to both miR-29 sites of the PTEN 3′ UTR (Figure S3B) (Hsin et al., 2018). Additionally, we used a miRNA mimic to overexpress miR-29 in mature B cells from C57BL/6 mice and observed a significant decrease in PTEN transcripts *in vitro* compared to controls (Figure S3C). Taken together, these results verified that miR-29 binds and targets both sites of the 3′ UTR of PTEN in B cells.

Increased PTEN Expression in miR-29 Null B Cells Leads to a Decrease in PI3K Signaling

In an effort to further characterize the role miR-29 plays in regulating BCR signaling *in vivo*, we examined the intracellular protein levels of the PI3K signaling cascade in B cells from DKO mice. An analysis of PTEN protein levels in B cells isolated from 4-week-old mice revealed a significant increase in PTEN levels (Figure S3D). In conjunction with B cell maturation, PTEN expression increased starting at the immature B cell stage and rose significantly above controls at the mature B cell stage (Figures S3E and S3F). Further analyses revealed that the increase in PTEN protein levels was most significant in FO B cells (Figure 2E), corresponding with miR-29 expression and the observed apoptosis pattern (Figures S1F and 2B). PI3K-dependent phosphorylation of phosphatidylinositol (4,5)-bisphosphate (PIP_2) to phosphatidylinositol (3,4,5)-triphosphate (PIP_3) recruits AKT to the plasma membrane where it is phosphorylated by PDK1 specifically at the Thr308 residue (Aiba et al., 2008; Okkenhaug and Vanhaesebroeck, 2003). Additional phosphorylation of AKT by the mammalian target of rapamycin (mTOR) at the Ser473 residue is necessary for signal transduction (Alessi et al., 1997; Sarbassov et al., 2005; Vanhaesebroeck et al., 2010). To examine the impact of the augmented PTEN expression on PI3K signaling in miR-29 null B cells, we examined the ratio of mean fluorescence intensity (MFI) of phosphorylated AKT (pAKT) to the MFI of total AKT (panAKT). The pAKT/panAKT ratio for Thr308 was significantly downregulated in FO B cells from DKO mice compared to controls (Figure 2F). Although not significantly downregulated, the pAKT/panAKT ratio for S473 was notably reduced in the miR-29 null FO B cells compared to controls (Figure 2F).

miR-29 Affects the B Cell End-Stage Fate Decision

When a FO B cell engages its cognate antigen, it can either form germinal centers and undergo class switch recombination or differentiate into a plasma cell. The decision to enter either fate is dependent on a host of factors, including the strength of the PI3K signal downstream of the engaged BCR (Limon and Fruman, 2012). As a regulator of PI3K signaling, various PTEN protein levels have been shown to affect end-stage fate decisions in B cells (Omori et al., 2006; Suzuki et al., 2003). To investigate if there are differences in

plasma cell differentiation for miR-29 null B cells, we first analyzed the percentage of plasma cells *in vivo*. Plasma cells reside in niches within the bone marrow as well as secondary lymphoid organs, such as the spleen. We observed a significant decrease in plasma cells in both the spleen and bone marrow of the DKO mice (Figures 3A and S4A). To examine differences in class switch recombination, we analyzed antibody titers in the sera of DKO and control mice. We observed a trending decrease in immunoglobulin M (IgM) and a significant increase in IgG1 antibodies in the DKO mice sera compared to controls (Figure 3B). *In vitro* stimulation of isolated FO B cells corroborated *in vivo* findings. DKO B cells demonstrated a decrease in plasma cell differentiation and an increase in class switch recombination to IgG1, IgG2A/2B, and IgA compared to controls, with a similar trend observed with single KO B cells (Figures 3C–3F, S4B, and S4C).

PTEN Haploinsufficiency Partially Rescues Phenotype

To rescue B cells in the periphery, we crossed our DKO mouse model onto a $PTEN^{fl/+}$ background (Lesche et al., 2002), limiting PTEN expression to one allele specifically in the miR-29-deficient B cells of our DKO mice (mb1Cre/+ miR-29ab1$^{fl/fl}$ miR-29b2c$^{-/-}$ PTEN $^{fl/+}$, from here on our referred to as DKO/bPTEN$^{+/-}$). Analyses of DKO/bPTEN$^{+/-}$ spleens revealed a dramatic increase in the frequency of B cells compared to the frequency of total B cells and FO B cells observed in the spleens of DKO mice (Figures 4A and 4B). Additionally, Annexin V and caspase staining demonstrated that the increased apoptosis in DKO B cells was reduced upon ablation of one *Pten* allele in DKO/bPTEN$^{+/-}$ mice (Figure 4C). However, although we observed a striking increase in the frequency of B cells in DKO/bPTEN$^{+/-}$ mice relative to DKO animals, the total numbers of B cells and FO B cells in the spleens DKO/bPTEN$^{+/-}$ mice were not significantly increased (Figures S5A and S5B). As mb1Cre/+ $PTEN^{fl/+}$ mice (bPTEN$^{+/-}$) exhibited a similar decrease in total B cells compared to controls, we reasoned that the loss of PTEN during B cell development affected B cell hematopoiesis. Indeed, the total number of pro-B cells was increased, whereas the total numbers of pre-B and immature B cells were decreased (albeit not significantly) in the bone marrow of both the bPTEN$^{+/-}$ and DKO/bPTEN$^{+/-}$ mice compared to controls (Figure S5C).

An analysis of the differentiation capacity of rescued B cells demonstrated that ablation of one copy of *Pten* in B cells devoid of miR-29 led to the normalization of plasma cell differentiation and class switch recombination (Figures 4D and 4E). Interestingly, *in vitro* analyses of B cells from bPTEN$^{+/-}$ mice revealed a decrease in plasma cell differentiation compared to controls. This finding contradicts studies done with CD19Cre/+ $PTEN^{fl/+}$ mice, suggesting that the diminution of PTEN during early B cell development may have an impact on the ability of the B cell to differentiate into a plasma cell in the periphery (Omori et al., 2006; Suzuki et al., 2003).

DISCUSSION

The regulation of the PTEN-PI3K axis by miRNAs at various stages of B cell hematopoiesis is crucial for establishing the appropriate BCR signaling strength as cells progress through development. Previous research has focused on miRNA-dependent PTEN regulation in early B cell development in the bone marrow. However, our understanding of the regulation of

PI3K signaling and PTEN by individual miRNAs in the periphery remains fragmentary. The identification of miR-29 as a key regulator of the PTEN-PI3K axis later in B cell development reveals a mechanism for RNAi-dependent control of survival and the end-stage fate decision of mature FO B cells.

In this study, we examined mouse models deficient for miR-29 miRNAs specifically in B cells to determine the impact that miR-29 ablation has on BCR signaling. An analysis of bone marrow B cells revealed no change in progenitor or immature B cell populations, suggesting that early B cell development was not affected in DKO mice. In the spleen, however, DKO mice exhibited a 3-fold reduction in total B cells that were verified to exhibit a diminution in miR-29 miRNAs compared with controls owing to a significant loss in FO B cells due to apoptosis. A similar loss was observed in a PTEN transgenic mouse model that exhibited a decrease in splenic mature B cells (Andrew Getahun, personal communication). PI3K signaling is vital for B cell survival. Disturbing the PI3K signaling cascade in B cells results in the loss of B cells by apoptosis (Kraus et al., 2004; Lam et al., 1997). Furthermore, dampened PI3K signaling has been previously demonstrated to lead to a loss in FO B cells while sparing MZ B cells (Pillai et al., 2005).

We found that miR-29 regulated PTEN at the mature B cell stage. miR-29 expression increased as the B cell matured, ultimately peaking at the mature FO B cell stage. Renilla/luciferase assays confirm that miR-29 targets the 3′ UTR of PTEN at the two highly conserved sites identified by the Targetscan algorithm. Additionally, Ago HITS-CLIP analyses of *in-vitro*-activated B cells from C57BL/6 mice confirm the binding of RISC to the 3′ UTR of PTEN. Cre-lox-dependent ablation of miR-29 resulted in an increase in the PTEN protein with a concomitant decrease in the activation of AKT in mature FO B cells. Although the decreases in pAKT/panAKT ratios were modest in miR-29 null B cells, given the importance of the PI3K signaling cascade on the survival of B cells (Okkenhaug, 2013; Srinivasan et al., 2009), we believe an inappropriately dampened PI3K signal in B cells could cause the apoptosis observed in DKO mice. Furthermore, the B cells that have undergone apoptosis may have exhibited a more dramatic decrease in PI3K signaling. Indeed, crossing our DKO mouse model onto a $PTEN^{fl/+}$ background rescued the percentage of B cells from apoptosis in the periphery with an increase in the percentage of FO B cells compared with controls. These findings establish a role for miR-29-dependent control of mature FO B cell survival by RNAi of the PTEN-PI3K axis downstream of the BCR.

Interestingly, the ablation of miR-29 in B cells had a profound effect on the end-stage fate decision of mature FO B cells. In the DKO mice model, we observed a significant decrease in plasma cells within the bone marrow and spleen of miR-29 null mice. Despite the reduction in plasma cell numbers, there was an increase in serum IgG1 with a concurrent decrease in IgM antibodies in the sera of DKO mice compared to controls. *In vitro* differentiation assays revealed that once activated, miR-29 null B cells preferentially underwent class switch recombination over differentiation into plasma cells. It has been well documented that altered PI3K signaling is associated with changes in plasma cell differentiation and class switch recombination efficiencies (Limon and Fruman, 2012; Omori et al., 2006; Suzuki et al., 2003). When one allele of *Pten* was ablated in our DKO B

cells, we observed a full rescue of the *in vitro* phenotypes, suggesting that PTEN dysregulation was responsible for the observed differences seen with miR-29 null B cells.

The present findings focus specifically on PTEN regulation, but as with most miRNAs, the pleiotropic effects of the miR-29 family are likely to influence a wide range of transcripts in B lymphocytes. Further research may provide insights into other networks and transcripts that contribute to the phenotypes observed upon the loss of miR-29 in B cells. Unfortunately, we could not confidently examine other differentially expressed transcripts in our miR-29 null B cells by conventional methods. Examining the B cells of our DKO mouse model would result in skewed results, as these B cells have selective pressures that have allowed them to escape apoptosis.

Additionally, our analyses of PTEN haploinsufficiency in B cells revealed results counter to published data. Prior studies focused on $PTEN^{fl/+}$ mice crossed onto a CD19Cre/+ background, which is expressed starting at the pre-B cell stage, and reported increases in total B cells numbers as well as augmented plasma cell differentiation (Anzelon et al., 2003; Omori et al., 2006; Suzuki et al., 2003). Our $bPTEN^{+/-}$mouse model took advantage of the mb1Cre gene, which is expressed starting at the pro-B cell stage (Hobeika et al., 2006), to ablate one allele of *Pten*. We observed an increase in pro-B cells with a concomitant decrease in pre- and immature B cells, indicating a partial block in early B cell hematopoiesis upon the loss of a single *Pten* allele. Furthermore, we observed a decrease in total splenic B cell numbers and diminished plasma cell differentiation in our $bPTEN^{+/-}$ mice compared to controls. These results suggest that the ablation of one allele of *Pten* earlier in B cell development impacts the survival of B cells in the periphery as well as the differentiation capacity of FO B cells. Although these findings raise questions related to PTEN-PI3K signaling in early B cell development, it is beyond the scope of this paper.

The inverse expression pattern of the miR-29 family of miRNAs to that of the essential miR-17~ 92 cluster as the B cell matures suggests a critical role for miR-29 in later stages of B cell development. In addition to its role in regulating PTEN expression and the survival of developing B cells in the bone marrow, the miR-17~92 cluster has also been shown to be an important oncomir in B cells. Generally, miRNAs are downregulated, and the 3′ UTR of mRNA targets are truncated in tumors (Lu et al., 2005; Mihailovich et al., 2015); however, the miR-17~92 cluster is upregulated in many malignancies (He et al., 2005). Perhaps the increased miR-29 expression as the B cell matures plays a protective role while still allowing for miRNA-dependent regulation of PTEN at the mature B cell stage. Indeed, it has been documented that miR-17~92 aids in the onset and the progression of myc-induced B cell lymphomas (He et al., 2005; Mihailovich et al., 2015; Mu et al., 2009); conversely, miR-29 has been reported to function in a tumor suppressive role and is downregulated by myc in various cancers (Gong et al., 2014; Mott et al., 2010; Zhang et al., 2012). Further studies are necessary to determine if this inverse correlation is instrumental in limiting the malignant transformation of mature B cells and if miR-29 could be a viable target for cancer therapeutics.

Our analysis of miR-29-deficient B cells suggests that miR-29-dependent regulation of PTEN is necessary for the survival and end-stage fate decision of mature B cells. This study

outlines a novel role for miR-29 in controlling the vital PTEN-PI3K axis downstream of the BCR and gives a deeper understanding of RNAi regulation in mature FO B cells.

STAR★METHODS

RESOURCE AVAILABILITY

Lead contact—Further information and requests for resources and reagents should be directed to and will be fulfilled by the Lead Contact, Dr. Sergei Koralov (Sergei.Koralov@nyumc.org).

Materials availability—psiCHECK2 plasmids generated in this study will be made available on request. Transfer may require completion of material transfer agreement.

miR-29ab1^{fl} and miR-29b2c KO mice were generated by research groups of Drs. Ansel/McManus and Dr. Croce respectively and can be obtained following completion of appropriate material transfer agreements.

Data and code availability—This study did not generate any new datasets or codes.

EXPERIMENTAL MODEL AND SUBJECT DETAILS

For mouse models, miR-29ab1$^{fl/fl}$ mice (obtained from Dr. Mark Ansel's lab) and miR-29b2c$^{-/-}$ mice (obtained from Dr. Jining Lu's lab) were bred with Mb1-cre (Hobeika et al., 2006) and PTEN^{fl} (Lesche et al., 2002). Both male and female mice were used for experiments. Littermates that carried either the appropriate floxed alleles with non-targeted miR-29b2c loci or the Mb1-cre allele in the absence of the floxed alleles with intact miR-29b2c loci were used as controls. Mice were housed and maintained in specific pathogen-free conditions at NYU School of Medicine in accordance with protocols approved by the NYU Animal Care and Usage Committee. Unless explicitly stated, mice were used between 6–10 weeks of age.

METHOD DETAILS

Plasmid construction—psiCHECK-2 plasmid backbones were kindly shared by Dr. Eva Hernando's laboratory. gblocks (IDT) with 5′ and 3′ *NotI* restriction sites were designed using the first 2kb of the murine PTEN 3′UTR with mutated gblocks incorporating the sequence CCCCAAA at Targetscan predicted miR-29 sites and purchased from Integrated DNA Technologies (Coralville, Iowa, USA). Following digestion of gblocks and psiCHECK-2 plasmids with *NotI*, the linear psiCHECK-2 plasmid was ligated with the PTEN 3′UTR gblocks using a T4 DNA ligase (Takara). Post transfection, positive clones were detected via ampicillin selection plates and sequence was validated using Macrogen (Rockville, MD, USA) sequencing services with submitted primers: LucPlasmid Rvs 1 (5′-CGAGGTCCGAAGACTCATTT-3′) and LucPlasmid Rvs 2 (5′-CAAACCCTAACCACCGCTTA-3′).

Luciferase reporter activity assay—Plasmid (100ng) and 50nmol/L miR-29a, miR-29b, miR-29c, or miR-100 (Dharmacon) were co-transfected using Lipofectamine 2000

(Invitrogen) in Plat-ES cells. Three replicates of each condition were used each time. Following 48 hr transfection, Renilla and luciferase activity were measured using a the Dual Glo Stop & Glo kit (Promega) and a FlexStation 3 (Molecular Devices) plate reader according to the dual luciferase reporting system instructions. Relative Renilla enzymatic activity was compared using the ratio of Renilla reniformis and firefly luciferase activity.

Flow cytometry and cell sorting—For surface staining and cell sorting, single cell suspensions from spleen or bone marrow were stained 15 min on ice with antibodies specific to murine B220, CD19, c-kit, CD25, CD93 (AA4.1), CD38, CD21, CD23, IgA, Streptavidin APC Conjugate (eBioscience), CD95 (Fas), CD138 (BD Biosciences), IgG1, IgG2A-2B (BD PharMingen), and IgM (m chain specific) (Jackson ImmunoResearch). Dead cells were excluded by DAPI staining (Sigma). Annexin V staining was done according to manufacturer's protocol (eBioscience). For intracellular staining, cells were surface stained and fixation/permeabilization buffers (eBioscience) protocol was followed. Intracellular antibody used was PTEN (Cell Signaling) followed by FITC conjugated anti-rabbit antibody (Jackson ImmunoResearch). For intracellular phosphoflow staining, cells were surface strained then fixed in 2% PFA for 30 min at RT and permeabilized with 90% methanol for 30–60 min on ice. Cells were washed in PBS then stained for AKT, Phospho-AKT Thr308 and Phospho-AKT Ser473 (Cell Signaling) followed by FITC conjugated anti-rabbit antibody (Jackson ImmunoResearch). Samples were analyzed on an LSR Fortessa cytometer or sorted using a FACS Aria II (BD Biosciences). Data were analyzed with FlowJo software (Tree Star).

miRNA and gene expression analysis by real-time PCR—Total RNA was extracted using mirVana miRNA Isolation Kit (Ambion). TaqMan microRNA assays (Applied Biosystems) were used for reverse transcription and detection of miRNA levels. The small RNA U6 was used for normalization. Further isolation of longer RNAs was done by RNA cleanup using the RNeasy Micro kit (QIAGEN). cDNA was synthesized from mRNA using SuperScript VILO (Invitrogen). Real-time PCR was performed using a StepOne Plus PCR system using SybrGreen master mix (Applied Biosystems).

ELISA assay—To detect the level of IgG1 and IgM antibodies in mice sera, 96 well ELISA F-bottom, clear, Microlon 600 (high binding) microplates (Greiner Bio-one) were coated with goat anti-mouse kappa-UNLB (Southern Biotech) and goat anti-mouse lambda-UNLB (Southern Biotech) antibodies at 2.5 μg/mL O/N at 4C. After washing with PBS (3X), coated plates were blocked with PBSA (PBS+0.5% BSA+0.01% azide) for 1 h at RT. Sera was added to plates at a serial dilution of 1:500, 1:1000, and 1:2000 and incubated at RT for 2 h. Plates were washed with PBS (4X) and anti-IgM-biotin or anti-IgG1-biotin (Southern Biotech) were added to wells at a final concentration of 1 μg/mL. Plates were washed with PBS (4X) and streptavidin-AP (Roche) was added to wells at 1:3000 for 1 h at RT. Plates were washed with PBS (3X) and 4-nitrophenyl phosphate (Sigma) substrate in Developing Buffer (Thermo Scientific) was added to wells. Reaction was detected by a FlexStation 3 (Molecular Devices) plate reader. Concentration of antibody in sera was determined by comparing OD to standard curve. Standard curves obtained by serial dilutions

(0.025 μg/mL, 0.00625 μg/mL...9.76×10^{-5} μg/mL, 2.44×10^{-5} μg/mL) of IgM and IgG1 antibodies (Southern Biotech).

B cell culture assays—Plasma cell differentiation and class switch recombination assays were completed with mature B cells from LNs isolated using CD43+ Dynabeads depletion (ThermoFisher) and were stained with CellTrace Violet dye (BD Bioscience) to track proliferation. 1×10^6 B cells were plated in 500 mL of plasma cell media with 20 μg/mL LPS (Sigma-Aldrich) for plasma cell differentiation or IgG2A/2B class switch recombination assays, 25 μg/mL IL-4 (R&D Systems) and 2 μg/mL anti-CD40 (eBioscience) for IgG1 class switch recombination assay, and 20 μg/mL LPS and 1 ng/mL TGF-β for IgA class switch recombination assay. Cultured cells were harvested on day 4 and differentiation/class switch efficiencies were assessed via FACS.

Lipofectamine miRNA transfection assay was completed with mature B cells from LNs isolated as above. Lipofectamine reagents were prepared to the specifications of the Lipofectamine RNAiMAX Transfection Reagent (Invitrogen) protocol with either 10 pmol of siGlo (Dharmacon) or 10pmol of mmu-miR-29c-Fl (Dharmacon). 1×10^6 B cells were plated in 500 mL of plasma cell media with either prepared siGlo or mmu-miR-29c lipofectamine reagents. Cultured cells were harvested on day 3 and transfection efficiencies as well as PTEN expression were assessed via FACS

QUANTIFICATION AND STATISTICAL ANALYSIS

Statistical analyses were performed using Prism 7.0 (GraphPad Software). Statistical test noted in figure legends. Data reported with $n > 3$ mice. A p value of < 0.05 was considered significant.

Supplementary Material

Refer to Web version on PubMed Central for supplementary material.

ACKNOWLEDGMENTS

We are grateful to Dr. Eva Hernando and Doug Hanniford for providing the psiCHECK-2 plasmid and hRluc/Luc assay protocol. We thank Dr. Getahun for insightful discussions and for sharing his results on related work with us. We thank NYU Medical Center Cytometry and Cell Sorting Core for assistance. We thank all members of the Koralov lab for regular discussions of the presented results and valuable input. The graphical abstract was created with BioRender.com by Dr. Borbet. Work in the Koralov lab was supported by the NIH (R21AI110830, R21AI137752, and R01HL125816), a pilot grant from the Colton Center for Autoimmunity, and a Binational Science Foundation grant. M.J.H. was funded by the NYU MSTP T32 grant (T32GM007308). Research in the K.M.A. lab was supported by NIH grants (P01HL107202 and R01HL109102). The D.M. lab was funded by The Israel Science Foundation (1408/13).

REFERENCES

Abdelrasoul H, Werner M, Setz CS, Okkenhaug K, and Jumaa H (2018). PI3K induces B-cell development and regulates B cell identity. Sci. Rep 8, 1327. [PubMed: 29358580]

Aiba Y, Kameyama M, Yamazaki T, Tedder TF, and rosaki T (2008). Regulation of B-cell development by BCAP and CD19 through their binding to phosphoinositide 3-kinase. Blood 111, 1497–1503. [PubMed: 18025150]

Alessi DR, James SR, Downes CP, Holmes AB, Gaffney PR, Reese CB, and Cohen P (1997). Characterization of a 3-phosphoinositide-dependent protein kinase which phosphorylates and activates protein kinase Balpha. Curr. Biol 7, 261–269. [PubMed: 9094314]

Anzelon AN, Wu H, and Rickert RC (2003). Pten inactivation alters peripheral B lymphocyte fate and reconstitutes CD19 function. Nat. Immunol 4, 287–294. [PubMed: 12563260]

Avery DT, Kane A, Nguyen T, Lau A, Nguyen A, Lenthall H, Payne K, Shi W, Brigden H, French E, et al. (2018). Germline-activating mutations in *PIK3CD* compromise B cell development and function. J. Exp. Med 215, 2073–2095. [PubMed: 30018075]

Benhamou D, Labi V, Novak R, Dai I, Shafir-Alon S, Weiss A, Gaujoux R, Arnold R, Shen-Orr SS, Rajewsky K, and Melamed D (2016). A c-Myc/miR17–92/Pten Axis Controls PI3K-Mediated Positive and Negative Selection in B Cell Development and Reconstitutes CD19 Deficiency. Cell Rep. 16, 419–431. [PubMed: 27346348]

Chen C-Z, Li L, Lodish HF, and Bartel DP (2004). MicroRNAs modulate hematopoietic lineage differentiation. Science 303, 83–86. [PubMed: 14657504]

Clayton E, Bardi G, Bell SE, Chantry D, Downes CP, Gray A, Humphries LA, Rawlings D, Reynolds H, Vigorito E, and Turner M (2002). A crucial role for the p110delta subunit of phosphatidylinositol 3-kinase in B cell development and activation. J. Exp. Med 196, 753–763. [PubMed: 12235209]

Coffre M, Benhamou D, Rieß D, Blumenberg L, Snetkova V, Hines MJ, Chakraborty T, Bajwa S, Jensen K, Chong MMW, et al. (2016). miRNAs Are Essential for the Regulation of the PI3K/AKT/FOXO Pathway and Receptor Editing during B Cell Maturation. Cell Rep. 17, 2271–2285. [PubMed: 27880903]

Cushing L, Costinean S, Xu W, Jiang Z, Madden L, Kuang P, Huang J, Weisman A, Hata A, Croce CM, and Lü J (2015). Disruption of miR-29 Leads to Aberrant Differentiation of Smooth Muscle Cells Selectively Associated with Distal Lung Vasculature. PLoS Genet. 11, e1005238. [PubMed: 26020233]

Engelman JA, Luo J, and Cantley LC (2006). The evolution of phosphate-dylinositol 3-kinases as regulators of growth and metabolism. Nat. Rev. Genet 7, 606–619. [PubMed: 16847462]

Fairfax KA, Kallies A, Nutt SL, and Tarlinton DM (2008). Plasma cell development: from B-cell subsets to long-term survival niches. Semin. Immunol 20, 49–58. [PubMed: 18222702]

Fruman DA, Snapper SB, Yballe CM, Davidson L, Yu JY, Alt FW, and Cantley LC (1999). Impaired B cell development and proliferation in absence of phosphoinositide 3-kinase p85alpha. Science 283, 393–397. [PubMed: 9888855]

Gong J-N, Yu J, Lin H-S, Zhang X-H, Yin X-L, Xiao Z, Wang F, Wang X-S, Su R, Shen C, et al. (2014). The role, mechanism and potentially therapeutic application of microRNA-29 family in acute myeloid leukemia. Cell Death Differ. 21, 100–112. [PubMed: 24076586]

He L, Thomson JM, Hemann MT, Hernando-Monge E, Mu D, Goodson S, Powers S, Cordon-Cardo C, Lowe SW, Hannon GJ, and Hammond SM (2005). A microRNA polycistron as a potential human oncogene. Nature 435, 828–833. [PubMed: 15944707]

Hobeika E, Thiemann S, Storch B, Jumaa H, Nielsen PJ, Pelanda R, and Reth M (2006). Testing gene function early in the B cell lineage in mb1-cre mice. Proc. Natl. Acad. Sci. USA 103, 13789–13794. [PubMed: 16940357]

Hoffman W, Lakkis FG, and Chalasani G (2016). B Cells, Antibodies, and More. Clin. J. Am. Soc. Nephrol 11, 137–154. [PubMed: 26700440]

Hsin J-P, Lu Y, Loeb GB, Leslie CS, and Rudensky AY (2018). The effect of cellular context on miR-155-mediated gene regulation in four major immune cell types. Nat. Immunol 19, 1137–1145. [PubMed: 30224821]

Kong G, Zhang J, Zhang S, Shan C, Ye L, and Zhang X (2011). Upregulated microRNA-29a by hepatitis B virus X protein enhances hepatoma cell migration by targeting PTEN in cell culture model. PLoS One 6, e19518. [PubMed: 21573166]

Koralov SB, Muljo SA, Galler GR, Krek A, Chakraborty T, Kanellopoulou C, Jensen K, Cobb BS, Merkenschlager M, Rajewsky N, and Rajewsky K (2008). Dicer ablation affects antibody diversity and cell survival in the B lymphocyte lineage. Cell 132, 860–874. [PubMed: 18329371]

Kraus M, Alimzhanov MB, Rajewsky N, and Rajewsky K (2004). Survival of resting mature B lymphocytes depends on BCR signaling via the Igalpha/beta heterodimer. Cell 117, 787–800. [PubMed: 15186779]

Krol J, Loedige I, and Filipowicz W (2010). The widespread regulation of microRNA biogenesis, function and decay. Nat. Rev. Genet 11, 597–610. [PubMed: 20661255]

Kwabi-Addo B, Giri D, Schmidt K, Podsypanina K, Parsons R, Greenberg N, and Ittmann M (2001). Haploinsufficiency of the Pten tumor suppressor gene promotes prostate cancer progression. Proc. Natl. Acad. Sci. USA 98, 11563–11568. [PubMed: 11553783]

Lai M, Gonzalez-Martin A, Cooper AB, Oda H, Jin HY, Shepherd J, He L, Zhu J, Nemazee D, and Xiao C (2016). Regulation of B-cell development and tolerance by different members of the miR-17~92 family microRNAs. Nat. Commun 7, 12207. [PubMed: 27481093]

Lam KP, Kühn R, and Rajewsky K (1997). In vivo ablation of surface immunoglobulin on mature B cells by inducible gene targeting results in rapid cell death. Cell 90, 1073–1083. [PubMed: 9323135]

Landgraf P, Rusu M, Sheridan R, Sewer A, Iovino N, Aravin A, Pfeffer S, Rice A, Kamphorst AO, Landthaler M, et al. (2007). A mammalian microRNA expression atlas based on small RNA library sequencing. Cell 129, 1401–1414. [PubMed: 17604727]

Lesche R, Groszer M, Gao J, Wang Y, Messing A, Sun H, Liu X, and Wu H (2002). Cre/loxP-mediated inactivation of the murine Pten tumor suppressor gene. Genesis 32, 148–149. [PubMed: 11857804]

Limon JJ, and Fruman DA (2012). Akt and mTOR in B Cell Activation and Differentiation. Front. Immunol 3, 228. [PubMed: 22888331]

Liston A, Papadopoulou AS, Danso-Abeam D, and Dooley J (2012). MicroRNA-29 in the adaptive immune system: setting the threshold. Cell. Mol. Life Sci 69, 3533–3541. [PubMed: 22971773]

Liu P, Cheng H, Roberts TM, and Zhao JJ (2009). Targeting the phosphoinositide 3-kinase pathway in cancer. Nat. Rev. Drug Discov 8, 627–644. [PubMed: 19644473]

Lu J, Getz G, Miska EA, Alvarez-Saavedra E, Lamb J, Peck D, Sweet-Cordero A, Ebert BL, Mak RH, Ferrando AA, et al. (2005). MicroRNA expression profiles classify human cancers. Nature 435, 834–838. [PubMed: 15944708]

Mihailovich M, Bremang M, Spadotto V, Musiani D, Vitale E, Varano G, Zambelli F, Mancuso FM, Cairns DA, Pavesi G, et al. (2015). miR-17–92 fine-tunes MYC expression and function to ensure optimal B cell lymphoma growth. Nat. Commun 6, 8725. [PubMed: 26555894]

Mott JL, Kurita S, Cazanave SC, Bronk SF, Werneburg NW, and Fernandez-Zapico ME (2010). Transcriptional suppression of mir-29b-1/mir-29a promoter by c-Myc, hedgehog, and NF-kappaB. J. Cell. Biochem 110, 1155–1164. [PubMed: 20564213]

Mu P, Han Y-C, Betel D, Yao E, Squatrito M, Ogrodowski P, de Stan-china E, D'Andrea A, Sander C, and Ventura A (2009). Genetic dissection of the miR-17~92 cluster of microRNAs in Myc-induced B-cell lymphomas. Genes Dev. 23, 2806–2811. [PubMed: 20008931]

Okkenhaug K (2013). Signaling by the phosphoinositide 3-kinase family in immune cells. Annu. Rev. Immunol 31, 675–704. [PubMed: 23330955]

Okkenhaug K, and Vanhaesebroeck B (2003). PI3K in lymphocyte development, differentiation and activation. Nat. Rev. Immunol 3, 317–330. [PubMed: 12669022]

Okkenhaug K, Bilancio A, Farjot G, Priddle H, Sancho S, Peskett E, Pearce W, Meek SE, Salpekar A, Waterfield MD, et al. (2002). Impaired B and T cell antigen receptor signaling in p110delta PI 3-kinase mutant mice. Science 297, 1031–1034. [PubMed: 12130661]

Omori SA, Cato MH, Anzelon-Mills A, Puri KD, Shapiro-Shelef M, Calame K, and Rickert RC (2006). Regulation of class-switch recombination and plasma cell differentiation by phosphatidylinositol 3-kinase signaling. Immunity 25, 545–557. [PubMed: 17000121]

Pillai S, Cariappa A, and Moran ST (2005). Marginal zone B cells. Annu. Rev. Immunol 23, 161–196. [PubMed: 15771569]

Ramadani F, Bolland DJ, Garcon F, Emery JL, Vanhaesebroeck B, Corcoran AE, and Okkenhaug K (2010). The PI3K isoforms p110alpha and p110delta are essential for pre-B cell receptor signaling and B cell development. Sci. Signal 3, ra60. [PubMed: 20699475]

Sarbassov DD, Guertin DA, Ali SM, and Sabatini DM (2005). Phosphorylation and regulation of Akt/PKB by the rictor-mTOR complex. Science 307, 1098–1101. [PubMed: 15718470]

Shen H, Li L, Yang S, Wang D, Zhong S, Zhao J, and Tang J (2016). MicroRNA-29a contributes to drug-resistance of breast cancer cells to adriamycin through PTEN/AKT/GSK3b signaling pathway. Gene 593, 84–90. [PubMed: 27523474]

Smith KM, Guerau-de-Arellano M, Costinean S, Williams JL, Bottoni A, Mavrikis Cox G, Satoskar AR, Croce CM, Racke MK, Lovett-Racke AE, and Whitacre CC (2012). miR-29ab1 deficiency identifies a negative feedback loop controlling Th1 bias that is dysregulated in multiple sclerosis. J. Immunol 189, 1567–1576. [PubMed: 22772450]

Spierings DC, McGoldrick D, Hamilton-Easton AM, Neale G, Murchison EP, Hannon GJ, Green DR, and Withoff S (2011). Ordered progression of stage-specific miRNA profiles in the mouse B2 B-cell lineage. Blood 117, 5340–5349. [PubMed: 21403133]

Srinivasan L, Sasaki Y, Calado DP, Zhang B, Paik JH, DePinho RA, Kutok JL, Kearney JF, Otipoby KL, and Rajewsky K (2009). PI3 kinase signals BCR-dependent mature B cell survival. Cell 139, 573–586. [PubMed: 19879843]

Stambolic V, Suzuki A, de la Pompa JL, Brothers GM, Mirtsos C, Sasaki T, Ruland J, Penninger JM, Siderovski DP, and Mak TW (1998). Negative regulation of PKB/Akt-dependent cell survival by the tumor suppressor PTEN. Cell 95, 29–39. [PubMed: 9778245]

Sun H, Lesche R, Li DM, Liliental J, Zhang H, Gao J, Gavrilova N, Mueller B, Liu X, and Wu H (1999). PTEN modulates cell cycle progression and cell survival by regulating phosphatidylinositol 3,4,5,-trisphosphate and Akt/protein kinase B signaling pathway. Proc. Natl. Acad. Sci. USA 96, 6199–6204. [PubMed: 10339565]

Suzuki A, Kaisho T, Ohishi M, Tsukio-Yamaguchi M, Tsubata T, Koni PA, Sasaki T, Mak TW, and Nakano T (2003). Critical roles of Pten in B cell homeostasis and immunoglobulin class switch recombination. J. Exp. Med 197, 657–667. [PubMed: 12615906]

Thorpe LM, Yuzugullu H, and Zhao JJ (2015). PI3K in cancer: divergent roles of isoforms, modes of activation and therapeutic targeting. Nat. Rev. Cancer 15, 7–24. [PubMed: 25533673]

Tumaneng K, Schlegelmilch K, Russell RC, Yimlamai D, Basnet H, Mahadevan N, Fitamant J, Bardeesy N, Camargo FD, and Guan K-L (2012). YAP mediates crosstalk between the Hippo and PI(3)K–TOR pathways by suppressing PTEN via miR-29. Nat. Cell Biol 14, 1322–1329. [PubMed: 23143395]

Vanhaesebroeck B, Guillermet-Guibert J, Graupera M, and Bilanges B (2010). The emerging mechanisms of isoform-specific PI3K signalling. Nat. Rev. Mol. Cell Biol 11, 329–341. [PubMed: 20379207]

Ventura A, Young AG, Winslow MM, Lintault L, Meissner A, Erkeland SJ, Newman J, Bronson RT, Crowley D, Stone JR, et al. (2008). Targeted deletion reveals essential and overlapping functions of the miR-17 through 92 family of miRNA clusters. Cell 132, 875–886. [PubMed: 18329372]

Wang S, Gao J, Lei Q, Rozengurt N, Pritchard C, Jiao J, Thomas GV, Li G, Roy-Burman P, Nelson PS, et al. (2003). Prostate-specific deletion of the murine Pten tumor suppressor gene leads to metastatic prostate cancer. Cancer Cell 4, 209–221. [PubMed: 14522255]

Wang J, Wang Y, Wang Y, Ma Y, Lan Y, and Yang X (2013). Transforming growth factor β-regulated microRNA-29a promotes angiogenesis through targeting the phosphatase and tensin homolog in endothelium. J. Biol. Chem 288, 10418–10426. [PubMed: 23426367]

Wilson RC, and Doudna JA (2013). Molecular mechanisms of RNA interference. Annu. Rev. Biophys 42, 217–239. [PubMed: 23654304]

Winter J, Jung S, Keller S, Gregory RI, and Diederichs S (2009). Many roads to maturity: microRNA biogenesis pathways and their regulation. Nat. Cell Biol 11, 228–234. [PubMed: 19255566]

Xiao C, Srinivasan L, Calado DP, Patterson HC, Zhang B, Wang J, Henderson JM, Kutok JL, and Rajewsky K (2008). Lymphoproliferative disease and autoimmunity in mice with increased miR-17–92 expression in lymphocytes. Nat. Immunol 9, 405–414. [PubMed: 18327259]

Zhang X, Zhao X, Fiskus W, Lin J, Lwin T, Rao R, Zhang Y, Chan JC, Fu K, Marquez VE, et al. (2012). Coordinated silencing of MYC-mediated miR-29 by HDAC3 and EZH2 as a therapeutic target of histone modification in aggressive B-Cell lymphomas. Cancer Cell 22, 506–523. [PubMed: 23079660]

Highlights

- miR-29 is a critical modulator of PI3K signaling and survival in mature B cells
- miR-29 controls the apoptosis of mature B cells by regulating the PTEN-PI3K axis
- miR-29 in B cells contributes to the regulation of terminal differentiation
- PTEN haploinsufficiency ameliorates phenotypes associated with miR-29-deficiency

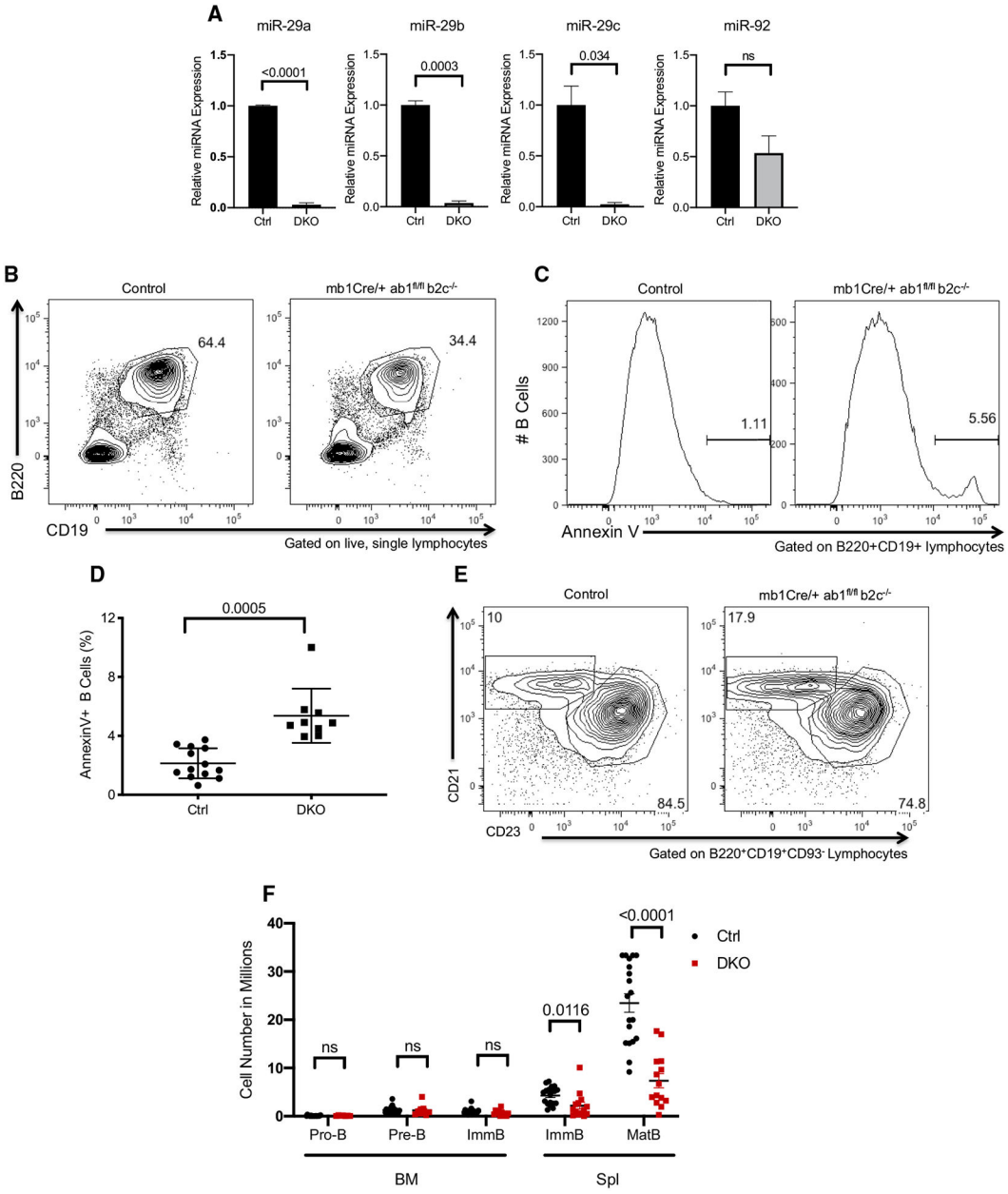

Figure 1. Decrease in Splenic miR-29 Null B Cell Populations Due to Apoptosis

(A) RT-PCR analyses of miR-29 and miR-92 miRNAs in splenic B cells isolated from control and DKO mice. Data are normalized to U6 and are represented relative to control cells (mean + SD indicated; three independent experiments). The p value is indicated when <0.05.

(B) Representative fluorescence-activated cell sorting (FACS) analysis of B220 and CD19 of spleens from control and DKO mice. Events are gated on live, total lymphocytes. Data are representative of >15 independent experiments.

(C) Representative Annexin V staining of splenic B cells ($CD19^+B220^+$) from control and DKO mice. Data are representative of >3 independent experiments.

(D) Frequency of Annexin-V-positive splenic B cells in control and DKO mice. Each dot is representative of one mouse; n ≥ 9 in each group (central horizontal bar indicates mean ± SD of >3 independent experiments). p value indicated.

(E) Representative FACS analysis of CD21 and CD23 of spleens from control and DKO mice. Events are gated on $B220^{+}CD19^{+}CD93^{-}$ splenocytes. Data are representative of >15 independent experiments.

(F) Total counts of labeled B cell populations from bone marrow and spleens of control (black dot) and DKO (red square) mice. Each dot is representative of one mouse; n ≥ 7 in each group (central horizontal bar indicates the mean ± SD of >3 independent experiments). The p value is indicated when <0.05.

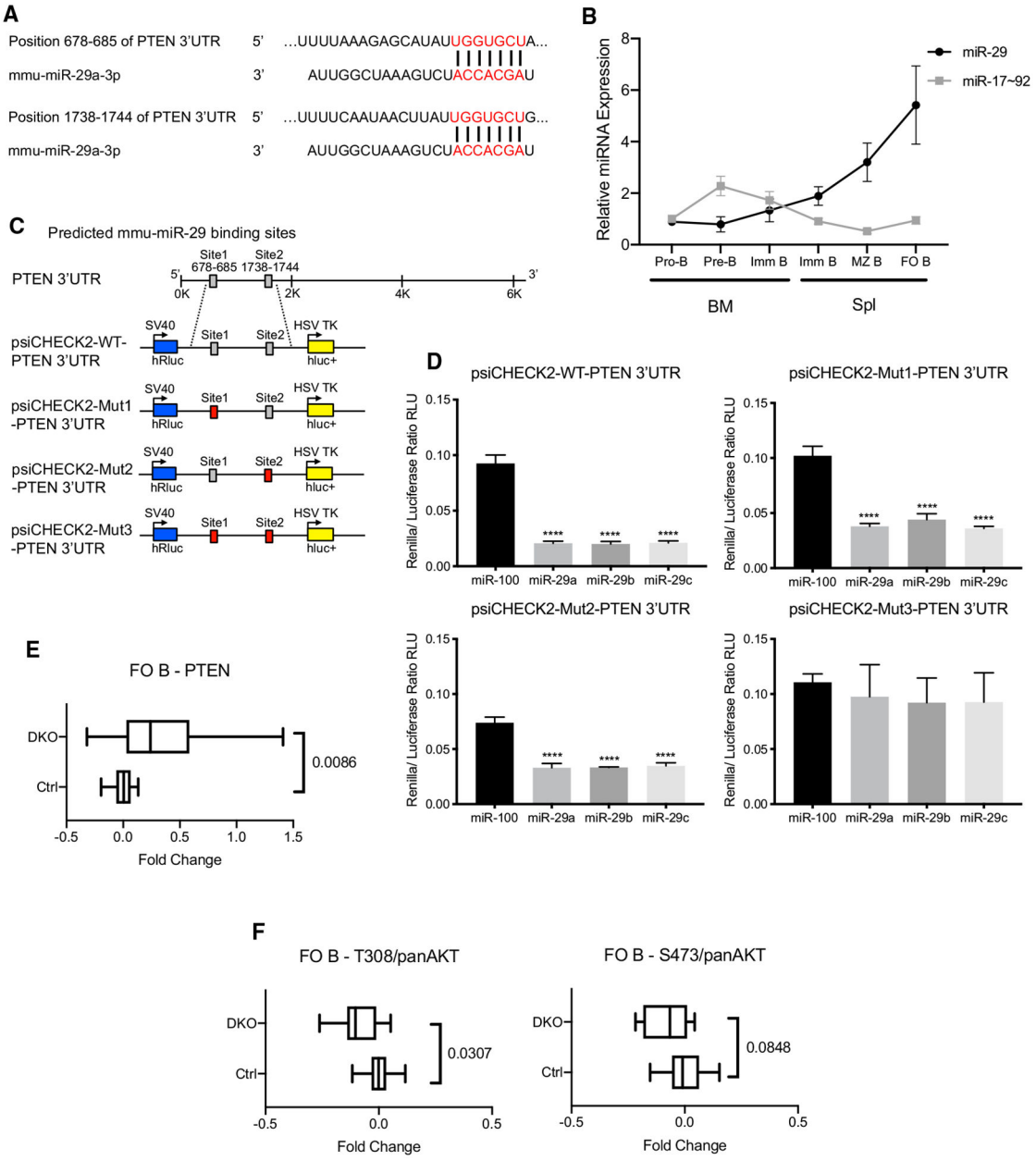

Figure 2. miR-29 Targets the 3′ UTR of PTEN, and miR-29 Ablation in B Cells Leads to Increased PI3K Signaling

(A) Predicted binding sites of miR-29a within the murine PTEN 3′ UTR at site 1 (position 678–685) and site 2 (position 1738–1744) by TargetScan. Seed region on miRNAs and targeted region on UTR are labeled in red.

(B) Averaged RT-PCR values of miR-29 (black line) and miR-17~92 (gray line) miRNAs of indicated sorted B cells from C57BL/6 mice. n = 3 mice. Data are normalized to U6 and represented relative to pro-B cells from each mouse. Data are presented as mean ± SD of triplicate replicates in 3 independent experiments.

(C) Schematic of miR-29 binding sites within the PTEN 3′ UTR and the corresponding sites within the psiCHECK2 plasmids containing the first 2 Kb of WT PTEN 3′ UTR or mutated

PTEN 3′ UTR inserted downstream of hRluc. Blue boxes indicate hRluc, and yellow boxes indicate hluc+. WT (gray boxes) and mutated (red boxes) miR-29 binding sites indicated. (D) Ratio of Renilla (hRluc)/luciferase (hluc+) activity with the indicated transfected plasmid and miRNA mimic. Results are presented as mean + SD (****$p < 0.0001$ as determined by Welch ANOVA test).

(E and F) Boxplot summarizing the fold change of PTEN (E) and the ratio of pAKT (T308 or S473)/panAKT (F) protein levels in splenic FO B cells of ~4-week-old DKO and control mice. Gated on $B220^{+}CD19^{+}CD93^{-}CD21^{mid}CD23^{+}$ splenocytes. Values of each population were calculated relative to the mean MFI from each experiment's control mice (fold change = $[(\text{sample} - \text{Control}_{mean})/\text{Control}_{mean}]$). The p value is indicated when <0.05, as determined by Mann Whitney test. $n \geq 6$ for each group from >3 independent experiments.

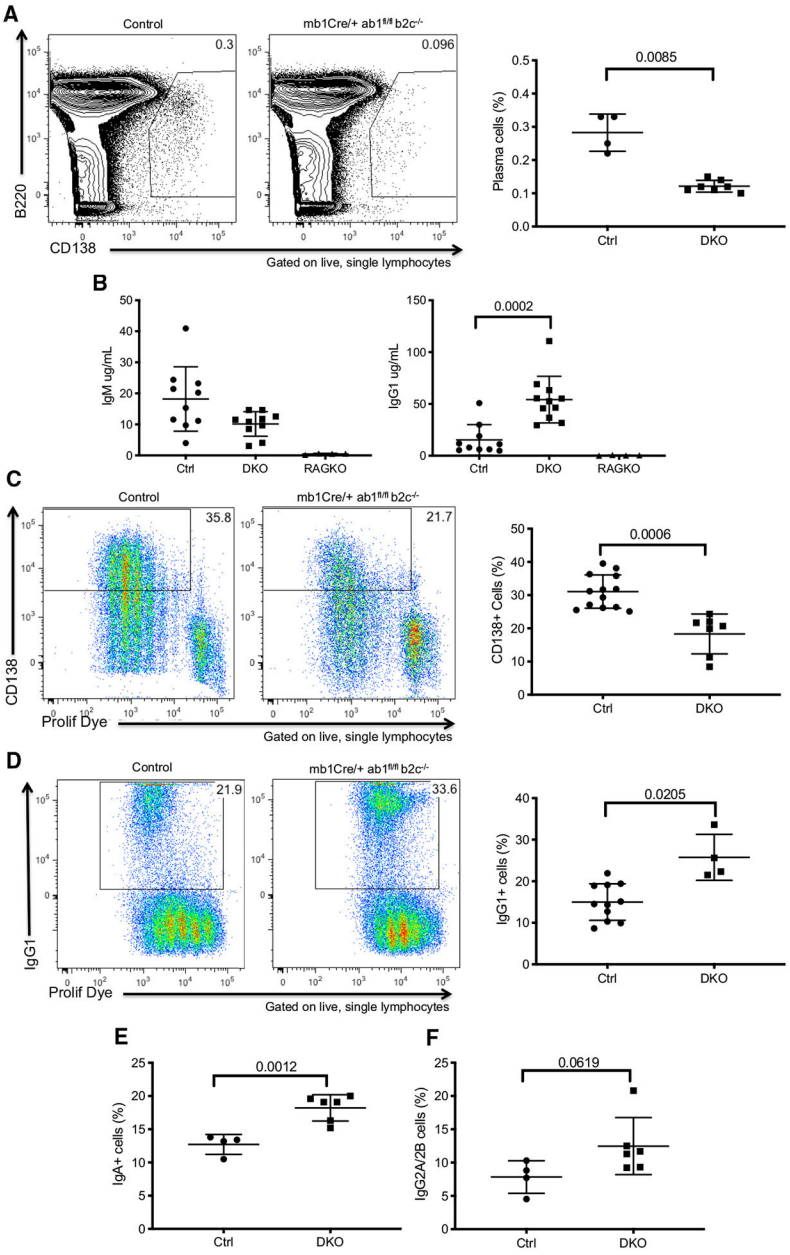

Figure 3. Decreased Plasma Cell Differentiation and Increased Class Switch Recombination in DKO Mice

(A) Representative FACS analysis (left) and percentage (right) of splenic plasma cells ($B220^{midlo}CD138^{+}$) from control and DKO mice. Each dot is representative of one mouse. n ≥ 4 for each group. Central horizontal bar indicates the mean ± SD. p value indicated.

(B) ELISA analysis of IgM and IgG1 levels in the sera of control, DKO, and recombination-activating gene knockout (RAGKO) mice. Each dot is representative of one mouse. n ≥ 4 for each group. Central horizontal bar indicates the mean ± SD of >3 independent experiments. The p value is indicated when <0.05.

(C) Representative FACS analysis (left) and percentage (right) of *in vitro*, lipopolysaccharide (LPS)-stimulated FO B cells with plasma cells labeled as $CD138^{+}$ from

control and DKO mice. Each dot is representative of one mouse. n ≥ 7 for each group. Central horizontal bar indicates the mean ± SD of >3 independent experiments. p value indicated.

(D) Representative FACS analysis (left) and percentage (right) of *in vitro* interleukin-4 (IL-4)- and CD40L-stimulated FO B cells with class-switched B cells labeled as $IgG1^+$ cells from control and DKO mice. Each dot is representative of one mouse. n ≥ 4 for each group. Central horizontal bar indicates the mean ± SD of >3 independent experiments. p value indicated.

(E) Percentage of *in vitro* LPS and transforming growth factor β (TGF-β)-stimulated FO B cells with class switched labeled as IgA^+ cells from control and DKO mice. Each dot is representative of one mouse. n ≥ 4 for each group. Central horizontal bar indicates the mean ± SD of >3 independent experiments. p value indicated.

(F) Percentage of *in vitro* LPS-stimulated FO B cells with class switched labeled as $IgG2A/2B^+$ cells from control and DKO mice. Each dot is representative of one mouse. n ≥ 4 for each group. Central horizontal bar indicates the mean ± SD. p value indicated.

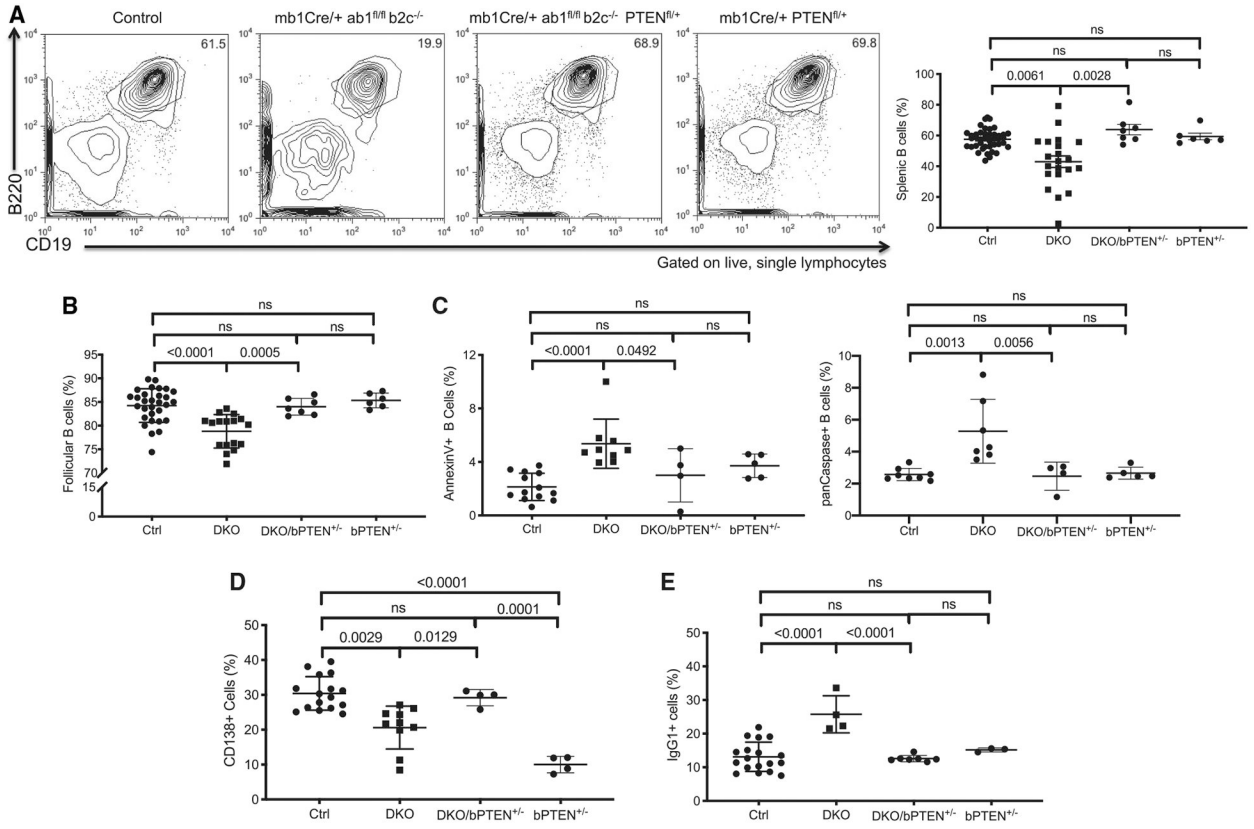

Figure 4. PTEN Haploinsufficiency Rescues DKO Phenotype

(A) Representative FACS analysis (left) and percentage (right) of B220 and CD19 of spleens from control, DKO, DKO/bPTEN$^{+/-}$, and bPTEN$^{+/-}$ mice. Events gated on live, total lymphocytes. Each dot is representative of one mouse. n ≥ 6 for each group. Central horizontal bar indicates the mean ± SD of >3 independent experiments. The p value is indicated when <0.05.

(B) Percentage of splenic FO B cells from control, DKO, DKO/bPTEN$^{+/-}$, and bPTEN$^{+/-}$ mice. Events gated on B220^{+}CD19^{+}CD93^{-}CD21^{mid}CD23^{+} splenocytes. Each dot is representative of one mouse. n ≥ 6 for each group. Central horizontal bar indicates the mean ± SD of >3 independent experiments. The p value is indicated when <0.05.

(C) Frequency of splenic B cells positive for Annexin V (left) and panCaspase (right) positive from control, DKO, DKO/bPTEN$^{+/-}$, and bPTEN$^{+/-}$ mice. Each dot is representative of one mouse. n ≥ 4 for each group. Central horizontal bar indicates the mean ± SD of >3independent experiments. The p value is indicated when <0.05.

(D) Percentage of *in vitro*, LPS-stimulated FO B cells with plasma cells labeled as CD138^{+} from control, DKO, DKO/bPTEN$^{+/-}$, and bPTEN$^{+/-}$ mice. Each dot is representative ofone mouse. n ≥ 4 for each group. Central horizontal bar indicates the mean± SD of >3 independent experiments. The p value is indicated when <0.05.

(E) Percentage of *in vitro* IL-4- and CD40L-stimulated FO B cells with class switched labeled as IgG^{+} cells from control, DKO, DKO/bPTEN$^{+/-}$, and bPTEN$^{+/-}$ mice. Each dot is

representative of one mouse. $n \geq 4$ for each group. Central horizontal bar indicates the mean ± SD of >3 independent experiments. The p value is indicated when <0.05.

KEY RESOURCES TABLE

REAGENT or RESOURCE	SOURCE	IDENTIFIER
Antibodies		
CD45R (B220) Monoclonal Antibody (RA3–6B2), PerCP-Cyanine5.5	eBioscience	Cat#45-0452-82; RRID: AB_1107006
CD19 Monoclonal Antibody (eBio1D3 (1D3)), PE-Cyanine7	eBioscience	Cat#25-0193-81; RRID: AB_657664
CD117 (c-Kit) Monoclonal Antibody (2B8), APC	eBioscience	Cat#17-1171; RRID: AB_469429
CD25 Monoclonal Antibody (PC61.5), PE	eBioscience	Cat#12-0251-83; RRID: AB_465608
CD93 (AA4.1) Monoclonal Antibody (AA4.1), APC	eBioscience	Cat#17-5892-82; RRID: AB_469466
CD38 Monoclonal Antibody (90), Alexa Fluor 700	eBioscience	Cat#56-0381-82; RRID: AB_657740
CD21/CD35 Monoclonal Antibody (eBio4E3 (4E3)), eFluor 450	eBioscience	Cat#48-0212-80; RRID: AB_2016634
Streptavidin APC Conjugate	eBioscience	Cat#17-4317-82
IgA Monoclonal Antibody (11-44-2), Biotin	eBioscience	Cat# 13-5994-82; RRID: AB_466863
Anti-Mouse CD23 PE-Cyanine7	eBioscience	Cat#25-0232-82; RRID: AB_469604
Biotin Rat Anti-Mouse IgG2a/2b	BD Biosciences	Cat#553398; RRID: AB_394836
PE-Cy7 Hamster Anti-Mouse CD95	BD Biosciences	Cat#557653; RRID: AB_396768
APC Rat anti-Mouse CD138	BD Biosciences	Cat#561705; RRID: AB_10896819
PE Rat Anti-Mouse IgG1	BD PharMingen	Cat#562027; RRID: AB_10894761
DAPI	Sigma	Cat#10236276001
Annexin V-FITC Apoptosis Detection Kit	eBioscience	Cat#BMS500FI; RRID: AB_2575598
PTEN (138G6) Rabbit mAb	Cell Signaling	Cat#9559; RRID: AB_390810
AKT Rabbit Anti-Mouse	Cell Signaling	Cat#9272; RRID: AB_329827
Phospho-AKT Thr308 Rabbit Anti-Mouse	Cell Signaling	Cat#13038; RRID: AB_2629447
Phospho-AKT Ser473 Rabbit Anti-Mouse	Cell Signaling	Cat#4060; RRID: AB_2315049
Goat anti-mouse lambda-UNLB	Southern Biotech	Cat#1060-01; RRID: AB_2794389
Goat anti-mouse kappa-UNLB	Southern Biotech	Cat#1050-01; RRID: AB_2737431
Anti-IgM-biotin	Southern Biotech	Cat#1020-08; RRID: AB_2737411
Anti-IgG1-biotin	Southern Biotech	Cat#1070-08; RRID: AB_2794413
Streptavidin-AP	Roche	Cat#1089161
IgM antibody	Southern Biotech	Cat#0101-01; RRID: AB_2629437
IgG1 antibody	Southern Biotech	Cat#0102-01; RRID: AB_2793845
Critical Commercial Assays		
T4 DNA ligase	Takara	Cat#6022
Lipofectamine 2000	Invitrogen	Cat#11668027
Dual Glo Stop & Glo kit	Promega	Cat# E2920
mirVana miRNA Isolation Kit	Ambion	Cat#AM1560
TaqMan microRNA assays	Applied Biosystems	Cat#4427975
RNeasy Micro kit	QIAGEN	Cat#74004
SuperScript VILO	Invitrogen	Cat#11754050
SybrGreen master mix	Applied Biosystems	Cat#4309155
CD43+ Dynabeads	ThermoFisher	Cat#11422D
Lipofectamine RNAiMAX Transfection Reagent – Delivery of siRNA	Invitrogen	Cat#13778075

REAGENT or RESOURCE	SOURCE	IDENTIFIER
CellTrace Violet Dye	BD Bioscience	Cat#C34557
Experimental Models: Organisms/Strains		
B6.C(Cg)-*Cd79a*$^{tm1(cre)Reth}$/EhobJ	The Jackson Laboratory	Stock No. 020505; RRID: IMSR_JAX:020505
miR-29ab1$^{fl/fl}$	This Paper	N/A
miR-29b2c$^{-/-}$	Smith et al., 2012	N/A
Oligonucleotides		
miR-29a mimic	Dharmacon	Cat#C-310521-07-0002
miR-29b mimic	Dharmacon	Cat#C-310382-05-0002
miR-29c mimic	Dharmacon	Cat#C-310522-07-0002
miR-100 mimic	Dharmacon	Cat#C-311316-00-0002
siGLO RISC-Free Control siRNA	Dharmacon	Cat#D-001630-01-05
mmu-miR-29c-Fl	Dharmacon	Cat#CTM-514288
Software and Algorithms		
FlowJo	Tree Star	N/A
Prism 7.0	Graphpad	N/A
Other		
Microlon 600 (high binding) microplates	Greiner Bio-one	Cat#675061
4-nitrophenyl phosphate substrate	Sigma	Cat#N2765
Developing Buffer	Thermo Scientific	Cat#34064